Lipids in Health and Disease

RESEARCH

Open Access

MG-132 activates sodium palmitate-induced autophagy in human vascular smooth muscle cells and inhibits senescence via the PI3K/AKT/mTOR axis

Zhiyun Shu[1,2], Xiangjun Li[2], Wenqing Zhang[2], Zixu Huyan[2], Dong Cheng[3], Shishun Xie[2], Hongyuan Cheng[2], Jiajia Wang[1] and Bing Du[1*]

Abstract

Objective This study aimed to reveal the role and mechanism of MG-132 in delaying hyperlipidemia-induced senescence of vascular smooth muscle cells (VSMCs).

Methods Immunohistochemistry and hematoxylin-eosin staining confirmed the therapeutic effect of MG-132 on arterial senescence in vivo and its possible mechanism. Subsequently, VSMCs were treated with sodium palmitate (PA), an activator (Recilisib) or an inhibitor (Pictilisib) to activate or inhibit PI3K, and CCK-8 and EdU staining, wound healing assays, Transwell cell migration assays, autophagy staining assays, reactive oxygen species assays, senescence-associated β-galactosidase staining, and Western blotting were performed to determine the molecular mechanism by which MG-132 inhibits VSMC senescence. Validation of the interaction between MG-132 and PI3K using molecular docking.

Results Increased expression of p-PI3K, a key protein of the autophagy regulatory system, and decreased expression of the autophagy-associated proteins Beclin 1 and ULK1 were observed in the aortas of C57BL/6J mice fed a high-fat diet (HFD), and autophagy was inhibited in aortic smooth muscle. MG-132 inhibits atherosclerosis by activating autophagy in VSMCs to counteract PA-induced cell proliferation, migration, oxidative stress, and senescence, thereby inhibiting VSMC senescence in the aorta. This process is achieved through the PI3K/AKT/mTOR signaling pathway.

Conclusion MG-132 activates autophagy by inhibiting the PI3K/AKT/mTOR pathway, thereby inhibiting palmitate-induced proliferation, migration, and oxidative stress in vascular smooth muscle cells and suppressing their senescence.

Keywords MG-132, Sodium palmitate, Hyperlipidemia, PI3K, Autophagy, Senescence, Atherosclerosis

*Correspondence:
Bing Du
dubing@jlu.edu.cn
[1]Department of Cardiology, First Hospital of Jilin University, Changchun, Jilin 130000, China
[2]Department of Experimental Pharmacology and Toxicology, School of Pharmaceutical Sciences, Jilin University, 1266 Fujin Rd, Changchun, Jilin 130000, China
[3]School of Medicine, South China University of Technology, Guangzhou 510006, China

Introduction

Vascular smooth muscle cells (VSMCs) are a fundamental component of the vascular wall and are primarily responsible for regulating vascular contraction and diastole, which controls vascular blood flow and blood pressure [1]. There is increasing evidence that VSMC senescence is one of the crucial factors affecting the occurrence and development of atherosclerosis (AS), and inhibiting VSMC senescence is considered to be an important strategy for the treatment of AS [2, 3].

Autophagy is a cellular self-regulatory process that maintains a stable internal cellular environment by breaking down and removing damaged proteins and organelles from the cell [4], which is intricately regulated by various factors such as nutritional status, energy metabolism, and cellular stress, and the PI3K/AKT/mTOR axis plays a pivotal role in this process. Phosphatidylinositol 3-kinase (PI3K) is a significant signal-transducing enzyme that phosphorylates phosphatidylinositol diphosphate (PI(4,5)P2) to phosphatidylinositol trisphosphate (PI(3,4,5)P3), which activates intracellular signaling pathways. Protein kinase B (AKT), a classical downstream molecule of PI3K, can activate the mammalian target of rapamycin (mTOR) via phosphorylation. mTORC1 phosphorylates its downstream molecules, which promotes protein synthesis and cell proliferation, and cell growth, metabolism, and survival [5–7]. Activation of the PI3K/AKT/mTOR signaling pathway can inhibit the initiation of autophagy, regulate the expression of autophagy-related genes, or inhibit the activity of autophagy-related signaling pathways [8–10].

Cellular senescence is the process by which the functional and metabolic activities of a cell gradually decrease, eventually leading to cell death. Recent studies have demonstrated a crucial correlation between senescence and autophagy in VSMCs, in which autophagy removes aged and damaged organelles, thereby attenuating the cellular senescence process [11]. As individuals age and adopt unhealthy dietary habits, the autophagic function of VSMCs progressively weakens, resulting in the accumulation of intracellular waste materials and compromised organelle function, thereby accelerating the senescence process [12, 13]. Consequently, enhancing autophagic activity in VSMCs may serve as a strategy to delay senescence onset and maintain vascular health.

MG-132 (Z-Leu-Leu-Leu-al) functions as a proteasome inhibitor, effectively impeding the protein hydrolysis activity of the 26 S proteasome complex, with an IC50 of 100 nM. The molecular structural formulae are depicted in Fig. 1. Moreover, MG-132 acts as a potent activator of autophagy, stimulating the autophagic pathway and mitigating the accumulation of intracellular debris and damaged organelles [14]. Therefore, it is hypothesized that MG-132 could impede atherosclerosis development and decelerate vascular aging. Further exploration of the underlying mechanism is imperative.

In this study, we aimed to investigate the effect of MG-132 on the senescence process of VSMCs induced by sodium palmitate (PA), to provide a theoretical basis for the development of MG-132 as a drug to delay AS.

Materials and methods

Experimental animals

SPF grade 30 8-week-old healthy male C57BL/6J mice (weight 20–22 g) were purchased from Changchun Fenglong Biotechnology Co. The experimental animals were kept in the Experimental Animal Centre of the First Hospital of Jilin University. All animal experiments were approved by the Ethics Committee for Animal Experiments of the First Hospital of Jilin University (NO.0845). The experiments were conducted according to the Regulations on the Administration of Laboratory Animals.

Main instruments and reagents

MG-132 was purchased from TergetMol (Shanghai, China). Pictilisib and Recilisib were purchased from MedChemExpress (Shanghai, China), ,sodium palmitate was purchased from sigma (Shanghai, China).A mouse immunohistochemistry (IHC) kit was purchased from Yeasen (Shanghai, China). Total cholesterol (TC), triglyceride (TG), low-density lipoprotein cholesterol (LDL-C), and high-density lipoprotein cholesterol (HDL-C) kits were purchased from Nanjing Jiancheng Bioengineering Institute (Nanjing, China). The Cell Autophagy Staining Assay Kit, Senescence β-Galactosidase Staining Kit, BeyoClick™ EDU-594 Cell Proliferation Assay Kit, and Reactive Oxygen Species Assay Kit were purchased from Beyotime (Shanghai, China). The 10% fetal lamb serum, 1% penicillin and streptomycin, Cell Counting Kit, BCA Protein Concentration Kit, RIPA Lysate, PMSF, Color Prestained Protein Molecular Weight Standard, and Universal Antibody Diluent were purchased from Seven (Beijing, China). DMEM (low glucose) medium, and Fetal Bovine Serum were purchased from Shanghai Zhong Qiao Xin Zhou Biotechnology Co. PI3K (R22768), p-PI3K (341468), AKT (342529), p-AKT (381555), mTOR (380411), p-mTOR (381557), ULK1 (381887), Beclin 1 (381896), OPN (R26171), α-SMA (R23450), NQO1 (381695), HO-1 (R24541), p21 (382492), P53 (345567), IL-1β (516288), TNF-α (346654) and GAPDH (380626) were purchased from ZenBio (Chengdu, China).Highsig ECL Western Blotting Substrate (Cat. No.:180–501; Tanon, Beijing, China).

Dosing reagent

Dissolve 200 mg of MG-132 in 2.1025 mL of DMSO to prepare a 200 mM MG-132 stock solution. Dilute the MG-132 stock solution with saline to 1 mg/kg for

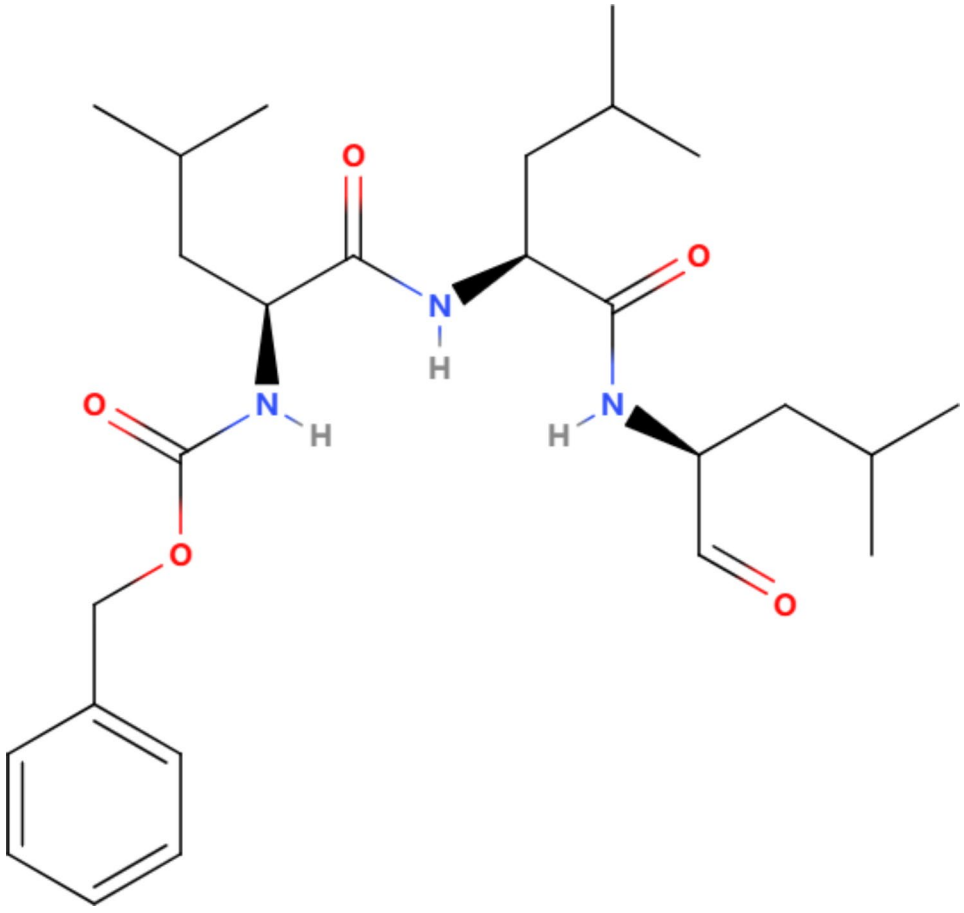

Fig. 1 Molecular Formula of MG-132

injection into mice. Dilute the MG-132 stock solution with DMEM to 40 μM. Dissolve 1 mg of Recilisib in 2.9692 mL of DMSO to prepare a 1 mM Recilisib stock solution. Dissolve 1 mg of Pictilisib in 1.9469 mL of DMSO to prepare a 1 mM Pictilisib stock solution. Dilute the Recilisib stock solution with DMEM to 50 μM and the Pictilisib stock solution to 2 nM. The DMSO concentration is less than 0.05% in all cases, thus excluding the influence of DMSO. The PA is dissolved in sterile PBS and heated at 70 °C. The PA is then added to 10% BSA for 5 min at 50 °C to give 20 mM PA.

Experimental methodology

Establishment and experimental grouping of the hyperlipidemic mouse model

The mice were randomly divided into 3 groups, the control group, the HF group, and the HF+MG-132 group, with 10 mice in each group. The normal control group was fed a normal diet, and the other groups were fed a high-fat diet. 5 weeks later, the mice in the MG-132 group were intraperitoneally injected with 1 mg/kg MG-132 per day, and those in the normal group and the model group were intraperitoneally injected with the same volume of saline. Each group was treated for 4 weeks.

TC, TG, LDL-C and HDL-C assays

After treatment the mice in each group were weighed every 3 days, blood was collected from the retro-orbital venous plexus once a week, and the serum was centrifuged at 4℃ and 3000 r/min. Total cholesterol (TC), triglycerides (TG), low-density lipoprotein cholesterol (LDL-C), and high-density lipoprotein cholesterol (HDL-C) were analyzed by an automatic biochemical analyzer.

Specimen collection

After completion of the experiment, the mice were anaesthetized and sacrificed by isoflurane inhalation, blood was collected from the heart apex, and then aortic tissues were removed and fixed in 4% paraformaldehyde solution for 96 h. After being rinsed and cleaned with saline, they were placed in a sealed box at -20 °C for storage.

Hematoxylin-eosin (HE) staining

The aortic tissues of each group, were subjected to paraformaldehyde and gradient sedimentary sugar

dehydration, paraffin embedding, slicing, baking, dewaxing with xylene and gradient ethanol, rehydration, and HE staining, After completion of the staining, the excess staining solution was removed, the tissues were dehydrated, cleared with xylene and sealed with neutral gum, and three randomly selected fields of view were observed for histopathological observation under the light microscope.

Immunohistochemical staining

Paraffin sections of each group of aortic tissues were sequentially subjected to dewaxing and hydration, antigen repair, blocking of endogenous peroxidase, serum closure, primary antibody incubation, rewarming, secondary antibody incubation, color development, hematoxylin restaining and sealing of the sections according to the manufacturer's instructions. The stained sections were observed and evaluated under a light microscope.

Cell culture and grouping

The VSMCs used in the study were purchased from Guangzhou Landm Biotechnology Co. All VSMCs used in the study were of the 10th generation. VSMC strains were kept in our research laboratory. Upon retrieval from liquid nitrogen, the VSMCs were cultured in serum-free medium supplemented with 10% fetal bovine serum, passaged, and utilized for experiments the following day once they reached a cell density of 90% in the culture dish. The experimental groups included: a control group - cultured in serum-free medium; a PA group - cultured in serum-free medium containing 40 μM PA; PA+MG-132 group - cultured in serum-free medium containing 40 μM PA and 40 μM MG-132; a PA+MG-132+Pictilisib group - cultured in serum-free medium containing 40 μM PA and 2 nM Pictilisib; and a PA+MG-132+Recilisib group cultured in serum-free medium containing 40 μM PA, 40 μM MG-132, and 50 μM Recilisib. The cells in each group were incubated for 24 h in the modified culture medium, after which the respective indices were measured.

CCK8 assay

VSMCs were cultured in 96-well plates (5×10^3 cells per well), and the cells were treated with different concentrations of PA and/or MG-132 for 24 h after cell adhesion. Subsequently, 20 μL of CCK8 reagent was added to each well, and the plates were incubated for another 30 min at 37 °C. The absorbance was measured using an enzyme-linked immunosorbent assay at a wavelength 570 nm.

EdU assay

VSMCs were inoculated into 6-well plates at an inoculum density of 5×10^5 cells/well. After 24 h of incubation in conditioned medium, 1 ml of fresh medium was added after the medium was aspirated. Subsequently, preheated EDU working solution was added and incubated for 2 h. After completing EdU labeling, the sections were fixed, washed, permeabilized, subjected to a click reaction and stained. Finally, fluorescence detection and imaging were performed.

Wound healing assay

A 6-well plate was inoculated with cells at a density of 5×10^5 cells/well. Pipette tips were placed vertically marked when the cell density reached more than 90%. The plates were incubated with serum-free medium supplemented with or without PA and MG-132 for 24 h. The VSMCs were observed and photographed at 0 and 24 h and the wound healing rate was determined by measuring the scratch area using ImageJ software.

Transwell cell migration assay

In the lower chamber, 700 μL of serum-free medium containing 10% FBS was added, while in the upper chamber, conditioned medium was added and resuspended, and 200 μL of VSMC cell suspension was collected for a total of 5×10^4 cells. The cells were incubated for 24 h under normal conditions and the cell chambers were washed with PBS and fixed with 4% paraformaldehyde. Finally, the cells were stained with 0.1% crystal violet for 10 min, rinsed and immersed in PBS several times, removed from the small chamber, the liquid was aspirated from the upper chamber, and the cells on the upper surface of the bottom membrane of the upper chamber were carefully removed with a wet cotton swab. The lower surface of the bottom membrane was observed under a microscope and photographed.

Autophagy staining assay

A 6-well plate was inoculated with cells at a density of 5×10^5 cells/well. The cells were cultured in conditioned medium for 24 h. After the medium was aspirated, 1 ml of monodansylcadaverine (MDC) staining solution was added to each well, and the cells were then cultured in a cell culture incubator at 37 °C for 30 min, protected from light. The MDC stain was aspirated and washed three times with assay buffer, using 1 ml of assay buffer each time. The assay buffer was aspirated, and 1 ml of assay buffer was added. The VSMCs were excited with UV light under a fluorescence microscope, green fluorescence was observed, and images were taken. The cells were observed for green fluorescence, and images were taken.

Reactive oxygen species assay

VSMCs were inoculated into 6-well plates at a density of 5×10^5 cells/well. The cells were cultured in conditioned medium for 24 h. After aspirating the medium, 1 ml of diluted DCFH-DA was added to each well and incubated

for 20 min in a cell culture incubator at 37 °C. The cells were washed three times with serum-free cell culture medium, excited with UV excitation light under a fluorescence microscope, after which the green fluorescence was observed and photographed.

Senescence β-Galactosidase staining

VSMCs were inoculated into 6-well plates at a density of 5×10^5 cells/well. The cells were cultured in conditioned medium for 24 h. after aspirating the medium, the cells were washed with PBS once, and 1 ml of β-galactosidase staining fixative was added, and fixed at room temperature for 15 min. the cell fixative was aspirated, and the cells were washed with PBS three times, each time for 3 min. the PBS was aspirated, and 1 ml of staining working solution was added to each well. the cells were incubated at 37℃ overnight, and then observed and photographed under the micro-scope.

Western blotting

Total cellular protein was extracted according to the kit instructions. After collection of the supernatant, total cellular proteins were quantified using the BCA protein content assay. The proteins were then denatured and inactivated in a metal bath at 95 °C for 5 min. Equal amounts of protein before electrophoresis were loaded onto a sodium dodecyl sulfate polyacrylamide gel and transferred to a polyvinylidene fluoride membrane using a transfer system. The membrane was blocked with 5% skim milk for one hour and incubated with the appropriate antibody overnight at 4 °C. Finally, the blot was incubated with an HRP-conjugated secondary antibody for one hour at room temperature in synergy with the blot. Immunoreactive proteins were photographed and visualized with enhanced chemiluminescence (ECL) solution. The band density in the images was quantified using Image J software.

Molecular docking validates the binding ability of MG-132 to PI3K

The 3D structure of MG-132 was retrieved through the PubChem website (https://pubchem.ncbi.nlm.nih.gov//), the spatial coordinates of the 3D structure in the SDF format file were downloaded, and the resulting SDF file was converted to the PDB for-mat by OpenBabel-2.4.1 software. The RCSB PBD database (https://www.rcsb.org/) was used to download the 3D structure of the PI3K protein in PDB format. Ligand molecules and water molecules were removed using PyMOL software. Next, molecular docking was performed using AutoDock Vina to verify the binding between the target and MG-132, and the optimal docking method was selected to visualize the results by PyMOL software.

Statistical analysis

All the statistical data are expressed as the mean ± standard deviation. One-way analysis of variance (ANOVA) was performed using SPSS 21 software (SPSS Inc., Chicago, IL, USA) and multiple comparisons were performed using the Newman-Keuls method. Images were analyzed using ImageJ software, and GraphPad Prism 9 was used for plotting. Statistical significance was set at $p<0.05$. The experiments were all repeated more than three times and the results are expressed as $\overline{x}\pm s$.

Results

MG-132 inhibits vascular structural transformation in hyperlipidaemic mice

The results demonstrated that hyperlipidemic mice, following continuous exposure to a high-fat diet exhibited a progressive increase in body weight over time, accompanied by elevated levels of total cholesterol (TC), triglycerides (TG), and low-density lipoprotein cholesterol (LDL-C), as well as a reduction in high-density lipoprotein cholesterol (HDL-C) concentration. Compared to those of high-fat (HF) group, the body weights of the HF + MG-132 group began to decrease beginning in the third week *(P<0.05)* but decreased significantly in the fourth week (*P<0.01*), despite no significant differences observed in the serum levels of TC, TG, LDL-C, and HDL-C (Fig. 2A and B).Histological analysis employing hematoxylin and eosin (HE) staining revealed that the thoracic aortic walls of mice in the HF group exhibited fractured elastic fibers, pronounced proliferation and disorganized arrangement of vascular smooth muscle cells, arterial wall thickening, and mild lipid deposition in specific arterial segments. These pathological alterations were mitigated to varying degrees in the HF + MG-132 group compared to those in the HF group (Fig. 2C).In conclusion, the administration of MG-132 in hyperlipidemic mice induced by a high-fat diet led to a reduction in body weight and amelioration of aortic wall lesions, suggesting a potential therapeutic benefit of MG-132 in attenuating the adverse effects of high-fat diet-induced hyperlipidemia.

MG-132 inhibits autophagy and senescence of VSMCs during arterial ageing in hyperlipidaemic mice

Immunohistochemical analysis revealed aberrant expression of p-PI3K, a key regulator of the autophagic process, in the HF group compared to the control group (*P<0.001*). Furthermore, the levels of the autophagy-associated proteins Beclin 1 and ULK1 were significantly reduced (*P<0.01*) in the HF group. In contrast, the HF + MG-132 group exhibited a significant decrease in p-PI3K expression compared to that in the HF group (*P<0.001*), accompanied by a notable increase in Beclin 1 and ULK1 expression (*P<0.01*). Moreover, significantly

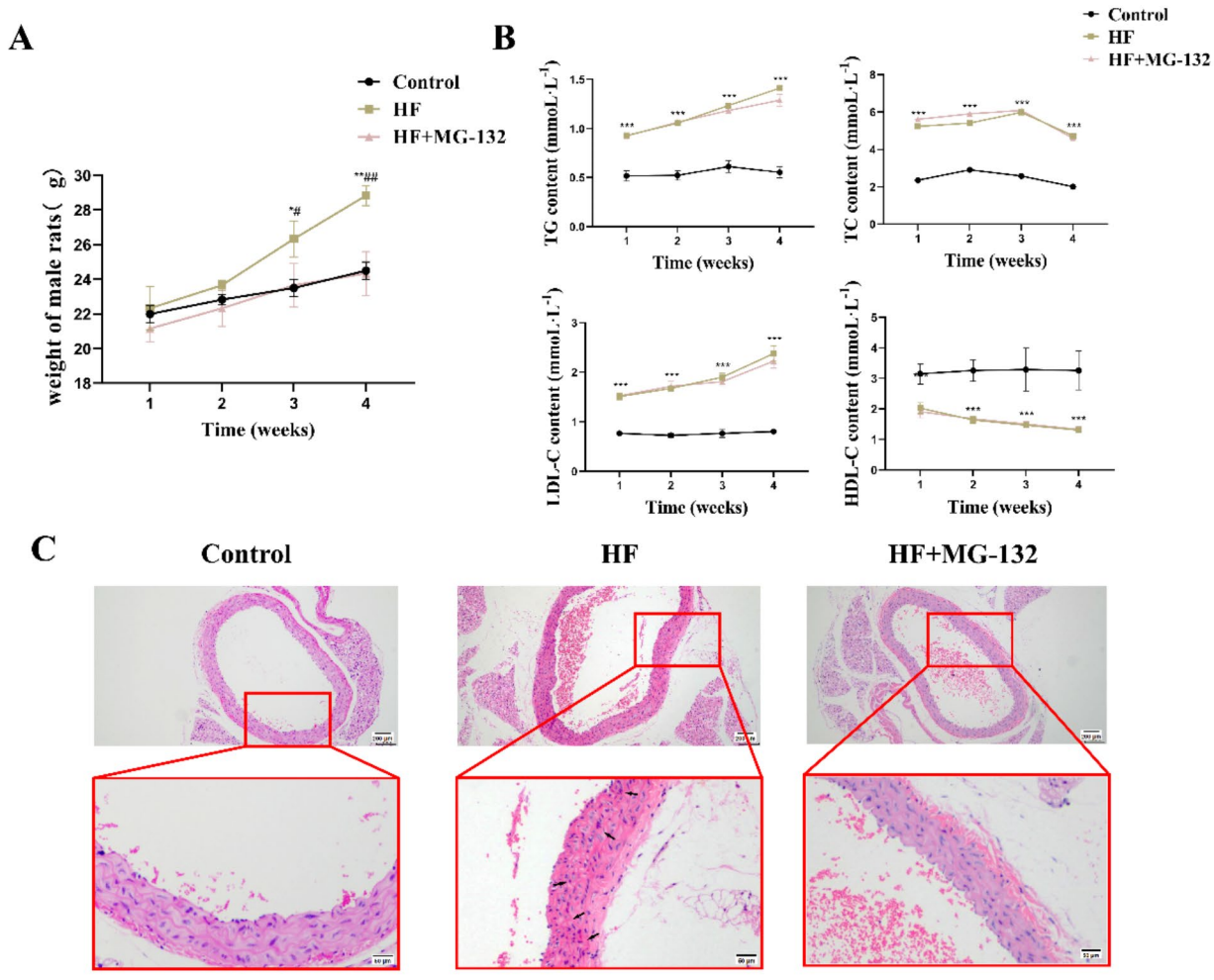

Fig. 2 MG-132 inhibits vascular structural transformation in hyperlipidaemic mice. (**A**) Changes in the body weight of mice with feeding time. $n = 10$. (**B**) serum TC, TG, LDL-C, and HDL-C levels in mic with feeding time. $n = 10$. (**C**) HE staining of mouse aorta, Scale bars = 200 μm, and 100 μm

greater levels of the vascular aging-related proteins p21 and p53, senescence-associated secretory phenotype (SASP) Markers (IL-1β and TNF-α) were detected in the HF group than in the control group ($P<0.001$), and these levels were significantly lower in the HF+MG-132 group than in the HF group ($P<0.01$). These preliminary findings hint at the potential of MG-132 to impact vascular aging and its association with arteriosclerosis by influencing vascular smooth muscle autophagy. Further investigations are warranted to elucidate the precise mechanism underlying this effect (Fig. 3).

Sodium palmitate promotes senescence of VSMCs

To study the effect of sodium palmitate on the proliferation of VSMCs, the CCK-8 and EdU assays were performed. The results of CCK-8 assay showed that the proliferation viability of VSMCs decreased continuously at 48 and 72 h of continuous PA induction, but induction of PA at different concentrations for 24 h resulted in a proliferation rebound of VSMCs. That is, the proliferation of VSMCs increased in a concentration dependent manner when the PA concentration exceeded 10 μM compared to 0 μM ($P<0.001$). Conversely, VSMC proliferation was significantly inhibited when the PA concentrations exceeded 320 μM ($P<0.001$, Fig. 4A). Excessive PA exposure may have profound effects on the physiological activity and morphological structure of VSMCs. In order to observe the early initial stage of cellular senescence before the onset of growth arrest,, PA concentrations of 10 μM and 40 μM were selected for subsequent experiments to evaluate the impact of PA on early VSMC senescence. The EDU assay results demonstrated a significant increase in VSMC EDU incorporation in the 10 μM and 40 μM PA groups compared to 0 μM PA group ($P<0.01$), indicating a dose-dependent response Fig. 4B).

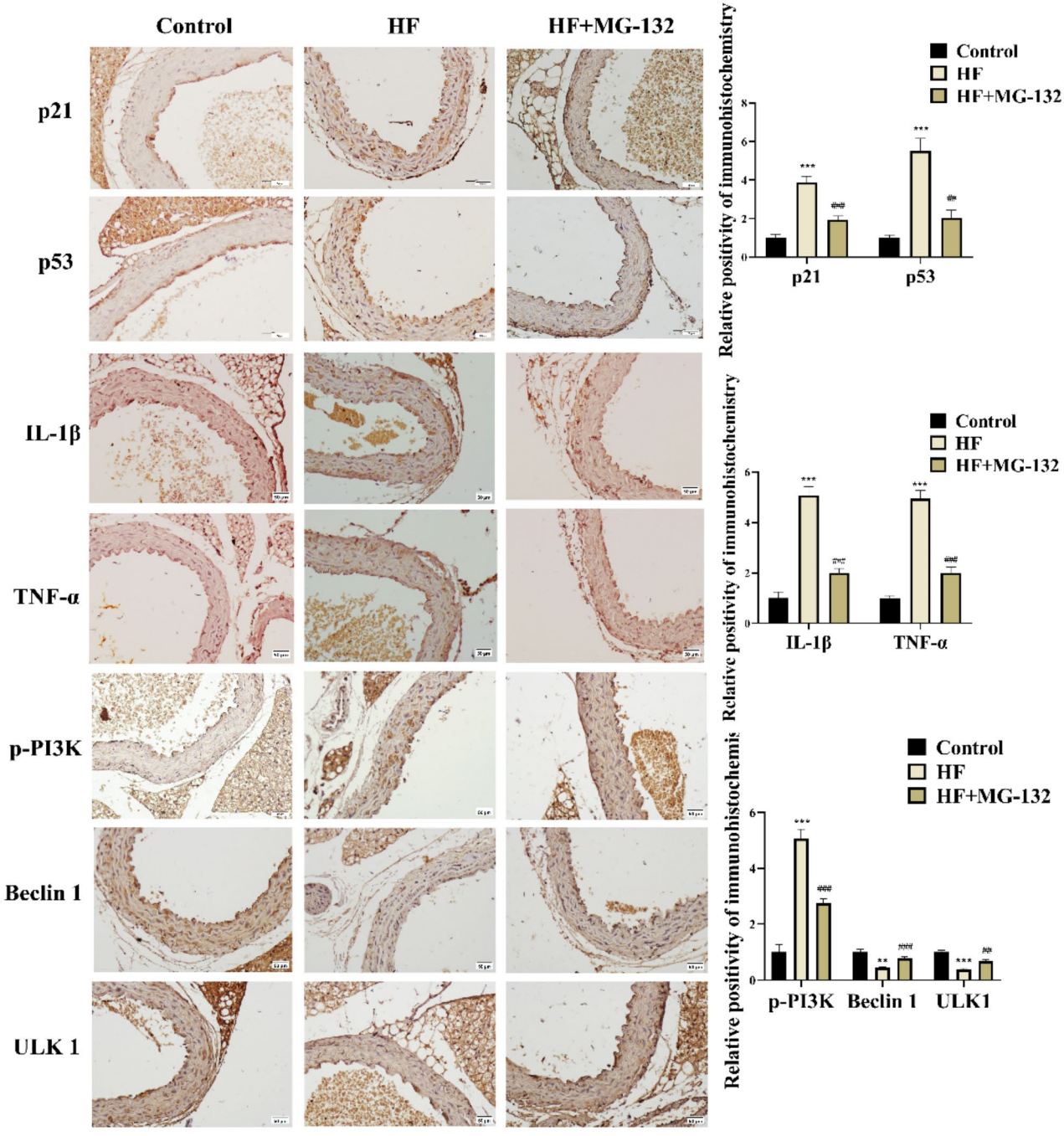

Fig. 3 MG-132 inhibits autophagy and senescence of VSMCs during arterial ageing in hyperlipidaemic. Immunohistochemistry analysis of p21, p53, IL-1β, TNF-α, p-PI3K, Beclin 1, and ULK1 in mouse aortas, Scale bars = 100 μm. $n = 10$. * $P < 0.05$, ** $P < 0.01$, *** $P < 0.001$ vs. Control; # $P < 0.05$, ## $P < 0.01$, ### $P < 0.001$ vs. HF

These findings further support that PA can stimulate VSMC proliferation.

To investigate the effect of sodium palmitate on the migratory capacity of VSMCs, wound healing and Transwell migration assays were performed. The results showed that PA treatment significantly increased the migration of VSMCs in a dose-dependent manner ($P < 0.05$,Fig. 4C and D).

The results of reactive oxygen species staining revealed a dose-dependent increase in oxidative stress levels in

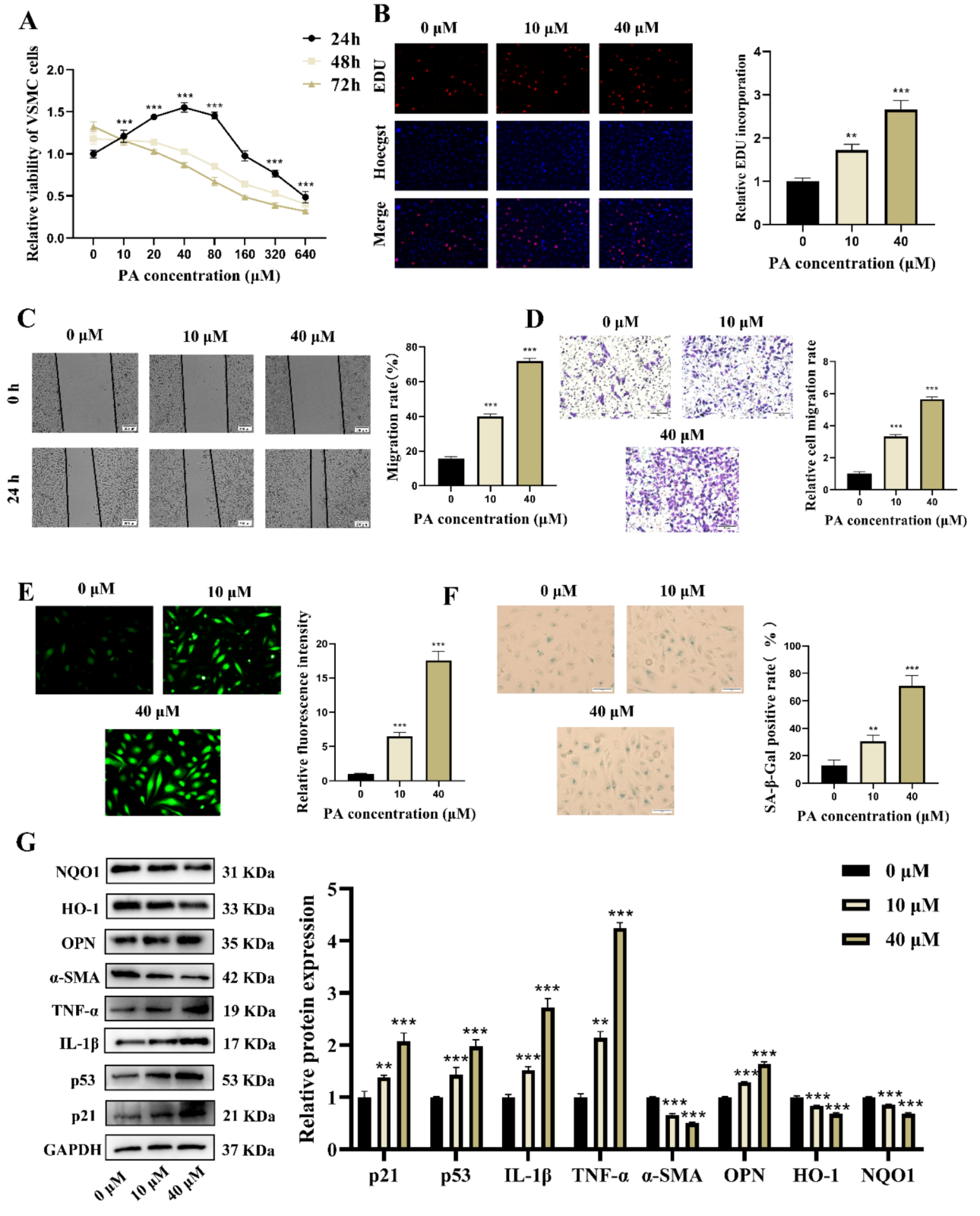

Fig. 4 (See legend on next page.)

(See figure on previous page.)

Fig. 4 Sodium palmitate promotes abnormal proliferation and migration of VSMCs, increases oxidative stress levels, and promotes senescence. (**A**, **B**) CCK-8 and EDU assays were used to assess the proliferative capacity of VSMCs. $n = 3$. (**C**) Wound healing assays were used to assess the migratory capacity of VSMCs. Scale bar = 200 μm. $n = 3$. (**D**) Transwell assays confirmed the migration-promoting effect of palmitic acid. Scale bar = 50 μm. (**E**) Reactive oxygen species staining used to assess the level of oxidative stress in VSMCs. $n = 3$. (**F**) β-galactosidase staining was used to assess the level of senescence in VSMCs. Scale bar = 50 μm. $n = 3$. (**G**) Western blotting was used to assess the expression of the senescence-associated proteins p21 and p53, senescence-associated secretory phenotype (SASP) Markers (IL-1β and TNF-α), the downregulation of the antioxidative stress proteins NQO1 and HO-1, the upregulation of the synthetic phenotypic marker OPN, and the downregulation of the contractile phenotypic marker α-SMA. All images were processed with ImageJ, and the data are expressed as the mean ± standard deviation, followed by the Newman-Keuls multiple comparison test. *$P < 0.05$, **$P < 0.01$, ***$P < 0.001$ *vs. PA (0 μM)*

VSMCs following PA treatment (*P<0.001*, Fig. 4E), as well as the downregulation of antioxidative stress proteins such as NQO1 and HO-1 (*P<0.001*), as detected by Western blot, indicating that PA was able to activate oxidative stress in VSMCs.

Furthermore, β-galactosidase staining demonstrated that PA induced VSMC senescence in a dose-dependent manner (*P<0.01*, Fig. 4F), Western blot analysis revealed that PA treatment significantly upregulation the expression of senescence-related proteins, including p21 and p53, senescence-associated secretory phenotype (SASP) Markers (IL-1β and TNF-α) (*P<0.01*), In addition, PA treatment decreased the expression of the contractile phenotypic marker α-SMA (*P<0.001*) and increased the expression of the synthetic phenotypic marker OPN (*P<0.001*, Fig. 4G). These findings provide further evidence that PA promotes VSMC senescence and phenotype changes.

Sodium palmitate inhibits autophagy in VSMCs via the PI3K/AKT/mTOR axis

To investigate the impact of sodium palmitate on cellular autophagy and its associated proteins, western blot and autophagy staining assays were performed. Western blot analysis revealed that PA treatment dose-dependently increased in the expression of the VSMC autophagy-related proteins p-PI3K/PI3K, p-AKT/AKT, and p-mTOR/mTOR (*P<0.05*), while the levels of ULK1 and Beclin 1 were dose-dependently reduced (*P<0.001*, Fig. 5A). Additionally, the results of the cellular autophagy staining assay demonstrated that PA dose-dependently inhibited the activation of autophagosomes in VSMCs (*P<0.001*,Fig. 5B). These findings suggest that PA can induce the phosphorylation of PI3K/AKT/mTOR, leading to mTOR axis phosphorylation and inhibition of autophagy in VSMCs.

MG-132 activates autophagy in VSMCs via PI3K

To investigate whether autophagy is activated in VSMCs by MG-132 via PI3K, PI3K was activated using Recilisib and inhibited using Pictilisib. Subsequently, the role of PI3K in the mechanism of action of MG-132 was examined. Western blot analysis revealed a significant decrease in the expression of the autophagy-related proteins p-PI3K/PI3K, p-AKT/AKT, and p-mTOR/mTOR in the VSMCs of the PA+MG-132 group (*P<0.001*). Conversely, compared with those in the PA+MG-132 group, the expression of ULK1 and Beclin 1 in the PA+MG-132 group VSMCs was significantly greater (*P<0.001*). Furthermore, in VSMCs from the PA+MG-132+Pictilisib group, the expression of the autophagy-related proteins p-PI3K/PI3K, p-AKT/AKT, and p-mTOR/mTOR was further decreased (*P*<0.001), while the expression of ULK1 and Beclin 1 was further increased (*P<0.001*). Interestingly, the PI3K activator Recilisib partially reversed the regulatory effect of MG-132 on autophagy-related proteins (*P<0.01*, Fig. 6A).

The results of the cellular autophagy staining assay demonstrated a significant increase in autophagosome activation of VSMCs in the PA+MG-132 group compared to the PA group (*P<0.001*). Moreover, compared with that in the PA+MG-132 group, the autophagosome activation of VSMCs in the PA+MG-132+Pictilisib group was further enhanced (*P<0.001*). Notably, Recilisib, a PI3K activator, reversed MG-132-induced autophagy in VSMCs (*P<0.001*, Fig. 6B), suggesting that PI3K plays a pivotal role in the activation of autophagy in VSMCs induced by MG-132.

MG-132 inhibits senescence of VSMCs through PI3K

To investigate whether VSMC proliferation could be inhibited by MG-132 through PI3K, CCK8 and EDU assays were conducted. The CCK-8 assay revealed a significant reduction in the proliferation of VSMCs in the PA+MG-132 group compared to that in PA group (*P<0.001*). Furthermore, the proliferation of VSMCs in the PA+MG-132 group was further decreased compared with that in the PA+MG-132+Pictilisib group (*P<0.001*). These findings suggest that MG-132 can suppress the aberrant proliferation of VSMCs and that this effect can be potentiated by the PI3K inhibitor Pictilisib. Conversely, the MG-132-induced inhibition of VSMC proliferation was reversed upon administration of the PI3K activator Recilisib (*P<0.001*,Fig. 7A). The results of the EdU assay confirmed that PI3K plays a crucial role in inhibiting the aberrant VSMC proliferation induced by MG-132 (Fig. 7B).

To investigate the impact of MG-132 on the migratory capacity of VSMCs via PI3K, wound healing and Transwell migration experiments were conducted. The results

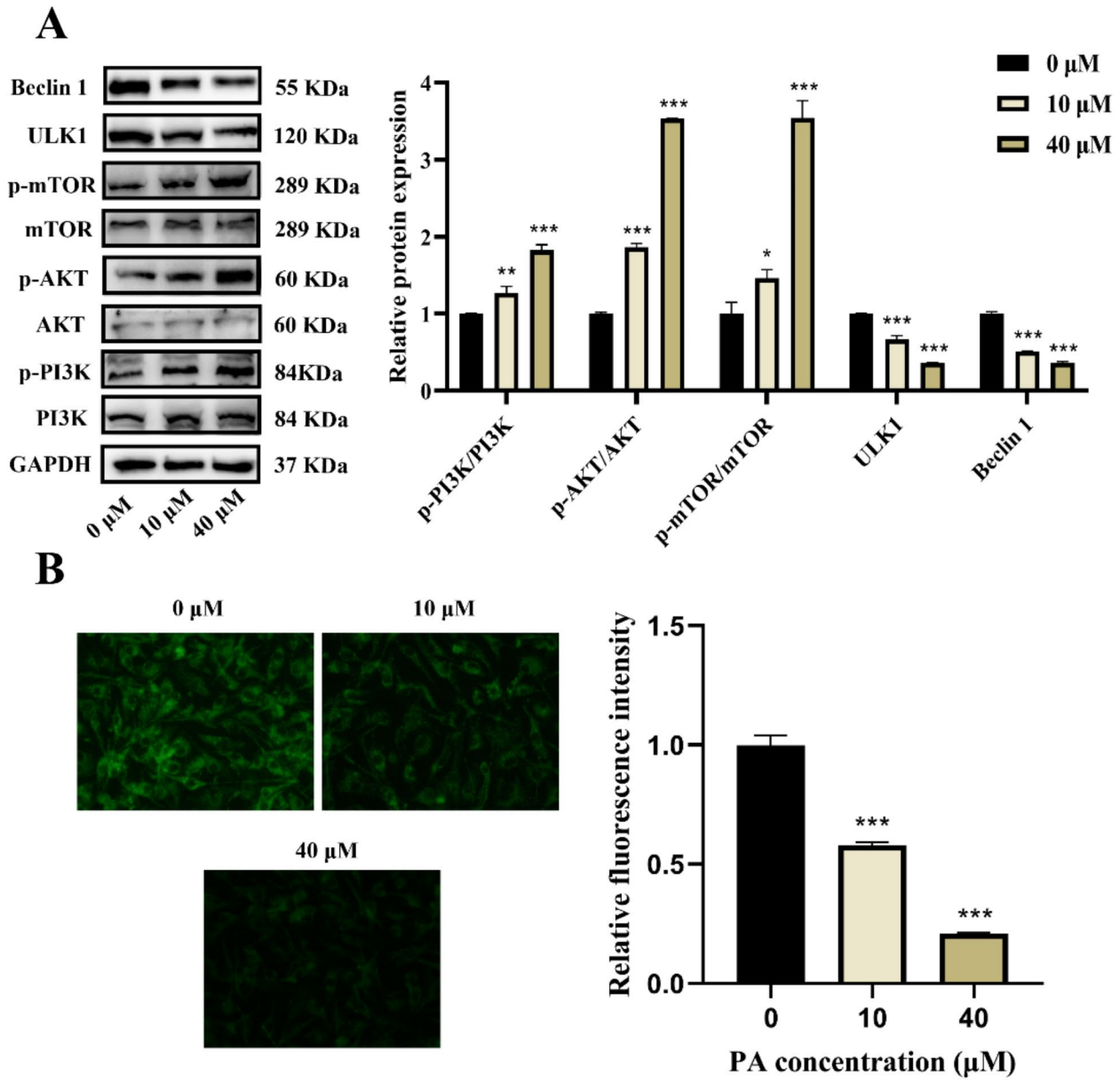

Fig. 5 Sodium palmitate promotes phosphorylation of PI3K/AKT/mTOR axis and inhibits autophagy in VSMCs. (**A**) Western blot analysis of the expression of the autophagy-related proteins p-PI3K /PI3K, p-AKT /AKT, p-mTOR/mTOR, ULK1, and Beclin 1 in VSMCs. $n = 3$. (**B**) Autophagy staining assay for evaluating the level of autophagy in VSMCs. $n = 3$. All images were processed with ImageJ and the data are expressed as mean ± standard deviation, followed by the Newman-Keuls multiple comparison test. *$P < 0.05$, **$P < 0.01$, ***$P < 0.001$ vs. PA(0 μM)

from the migration and Transwell assays demonstrated a significant reduction in the migratory ability of VSMCs in the PA+MG-132 group compared to that in the PA group ($P<0.001$). Additionally, the migratory capacity of VSMCs in the PA+MG-132+Pictilisib group was further diminished compared to that in the PA+MG-132 group ($P<0.01$). Interestingly, treatment with the PI3K activator Recilisib reversed the inhibitory effect of MG-132 on VSMC migratory ability ($P<0.001$, Fig. 7C and D).

The potential inhibitory effect of MG-132 on oxidative stress in VSMCs through the PI3K pathway was investigated by performing a reactive oxygen species staining assay. The results of the reactive oxygen species assay revealed a significant reduction in oxidative stress levels in VSMCs treated with PA+MG-132 compared to those in the PA group ($P<0.001$). Interestingly, further reductions in oxidative stress levels were observed in VSMCs treated with Pictilisib compared to those in VSMCs in

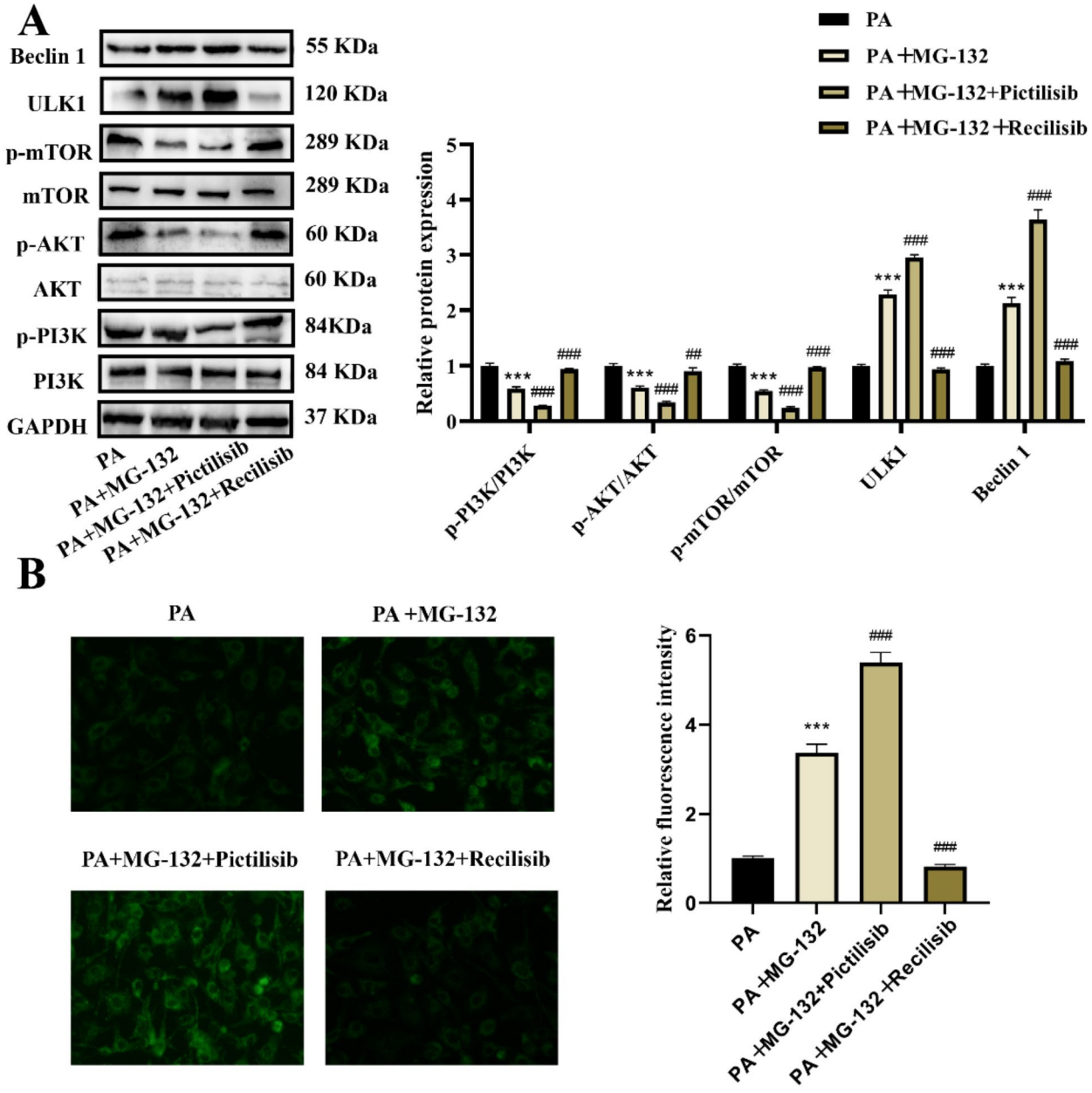

Fig. 6 MG-132 promotes autophagy in VSMCs induced by sodium palmitate via PI3K. (**A**) Western blot analysis of the expression of the autophagy-related proteins p-PI3K /PI3K, p-AKT /AKT, p-mTOR/mTOR, ULK1, and Beclin 1 in VSMCs. $n=3$. (**B**) Autophagy staining assay for evaluating the level of autophagy in VSMCs. $n=3$. All images were processed with Image J volume and the data were expressed as mean ± standard deviation, followed by Newman-Keuls multiple comparison test. ** P < 0.05, ** P < 0.01, *** P < 0.001 vs. PA; ## P < 0.01, ### P < 0.001 vs. PA + MG-132*

the PA+MG-132 group ($P<0.001$). Moreover, the addition of the PI3K activator Recilisib reversed the effect of MG-132 on oxidative stress levels in VSMCs ($P<0.001$, Fig. 7E). Western blot results showed that the expression of the antioxidative stress proteins NQO1 and HO-1 was significantly elevated in VSMCs in the PA+MG-132 group compared to those in the PA group ($P<0.001$), and the expression of NQO1 and HO-1 was further increased in the VSMCs in the PA+MG-132+Pictilisib group ($P<0.01$). However, Recilisib was able to inhibit the expression of these genes.

Furthermore, compared with that in the PA group, β-galactosidase staining significantly decreased the area of positive staining in the VSMCs treated with PA+MG-132 ($P<0.001$). Notably, the area of positively stained VSMCs in the PA+MG-132+Pictilisib group was further reduced compared to that in the PA+MG-132 group ($P<0.01$). Importantly, the PI3K activator Recilisib

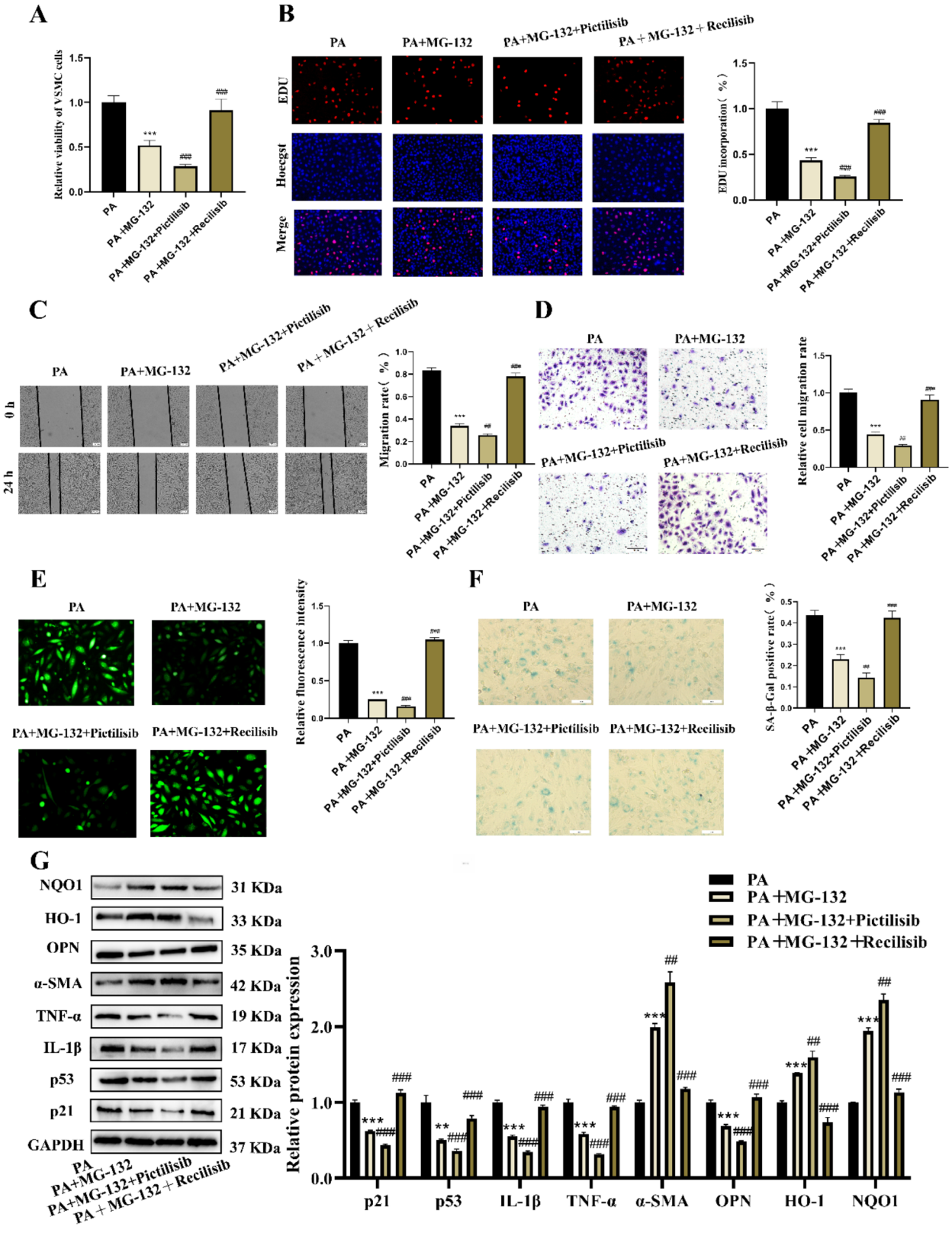

Fig. 7 (See legend on next page.)

(See figure on previous page.)

Fig. 7 MG-132 inhibits aberrant proliferation, migration and oxidative stress of VSMCs via PI3K and delays senescence. (**A**, **B**) CCK-8 and EDU assays were used to assess the proliferative capacity of VSMCs. $n=3$. (**C**) Wound healing assays were used to assess the migratory capacity of VSMCs. Scale bar = 200 μm. $n=3$. (**D**) Transwell assays confirmed the migration-promoting effect of palmitic acid. Scale bar = 50 μm. (**E**) Reactive oxygen species staining used to assess the level of oxidative stress in VSMCs. $n=3$. (**F**) β-galactosidase staining was used to assess the level of senescence in VSMCs. Scale bar = 50 μm. $n=3$. (**G**) Western blotting was used to assess the expression of the senescence-associated proteins p21 and p53, **senescence-associated secretory phenotype (SASP) Markers (IL-1β and TNF-α)**, the downregulation of the antioxidative stress proteins NQO1 and HO-1, the upregulation of the synthetic phenotypic marker OPN, and the downregulation of the contractile phenotypic marker α-SMA. All images were processed with ImageJ, and the data are expressed as the mean ± standard deviation, followed by the Newman-Keuls multiple comparison test. *$P<0.05$,**$P<0.01$,***$P<0.001$ *vs. PA;* #$P<0.05$,##$P<0.01$,###$P<0.001$ *vs. PA + MG-132*

reversed the effect of MG-132 on β-galactosidase staining in VSMCs ($P<0.001$, Fig. 7F). Western blotting revealed that the expression of the senescence-associated proteins p21 and p53, senescence-associated secretory phenotype (SASP) Markers (IL-1β and TNF-α) in VSMCs was significantly decreased in the PA + MG-132 group ($P<0.001$), and PA + MG -132 + Pictilisib further decreased the expression of p21 and p53, senescence-associated secretory phenotype (SASP) Markers (IL-1β and TGF-β) in VSMCs ($P<0.001$), and compared with the PA group, the PA + MG-132 group exhibited increased expression of α-SMA, a contractile phenotype marker ($P<0.01$), and suppressed expression of OPN, a synthetic phenotype marker, Additionally, Pictilisib further increased the expression of α-SMA, and Pictilisib further suppressed the expression of OPN ($P<0.01$); however, when we treated VSMCs with Recilisib, a PI3K activator, the expression of these senescence-related proteins significantly increased ($P<0.001$), whereas the expression of the contractile phenotypic marker α-SMA decreased ($P<0.001$) and the expression of the synthetic phenotypic marker OPN increased ($P<0.001$,Fig. 7G), suggesting that PI3K plays a key role in the inhibitory effects of MG-132 on senescence and phenotypic transformation in VSMCs.

Molecular docking validated the interaction of MG-132 with PI3K

The molecular docking results showed that the binding energy of MG-132 to PI3K was −7.7 kcal mol^{-1}, the ligand carbon atoms of MG-132 formed hydrophobic interactions with the PI3K amino acid residues GLU, TYR, LYS, LEU, and ILE, and the distances between the interacting carbon atoms were 3.88, 3.74, 3.72, 3.55, and 3.78, respectively. The MG-132 provided acceptor atoms to form hydrogen bonds with donor atoms provided by PI3K amino acid residue ARG, with a hydrogen atom to acceptor atom distance of 2.33, a donor to acceptor atom distance of 3.29, and a donor angle of 163.43 (Fig. 8). The above results indicate that there is a strong interaction between MG-132 and PI3K, and that PI3K may be a direct target of MG-132.

Discussion

The results of this research suggested that MG-132 can directly target PI3K, inhibit the AKT/mTOR pathway, activate autophagy in VSMCs, suppress cell proliferation and migration, reduce oxidative stress levels, modulate intracellular homeostasis, and delay senescence in VSMCs by inhibiting high-fat-induced phosphorylation of PI3K (Fig. 9, as illustrated by Figdraw). This finding provides new insights into the role of autophagy in VSMC senescence and suggests that manipulating cellular autophagy could represent a novel therapeutic strategy for treating human cardiovascular diseases associated with atherosclerosis.

High concentrations of free fatty acids (FFAs) due to disorders of fatty acid metabolism are direct triggers of atherosclerosis, ultimately leading to thickening, hardening and plaque formation in the vessel wall. In food, palmitic acid is the main source of saturated fatty acids among free fatty acids [15, 16]. Excessive consumption of foods with high palmitic acid content can cause elevated blood lipids, which ultimately leads to cardiovascular diseases such as AS [17–20]. In this study, C57BL/6J mice were fed high-fat chow, and after five consecutive weeks of feeding, the serum levels of TC, TG, and LDL-C were significantly elevated, HDL-C levels were significantly reduced, and elastic fiber rupture, the number of VSMC increasing, and the arterial wall thickened can be found in the thoracic aortic wall of the mice, Whereas the arterial wall of the mice given MG-132 showed that mild lipid deposition. In vitro culture of VSMCs treated with sodium palmitate for 24 h revealed that the cell proliferation, migration and oxidative stress were significantly increased, while the addition of MG-132 significantly decreased cell proliferation, migration and oxidative stress. These results indicated that MG-132 could inhibit the proliferation and migration of VSMCs, attenuate high-fat diet-induced aortic lesions, which maybe inhibit the occurrence and development of hyperlipemia and atherosclerosis.

Recent studies have shown that the metabolism of palmitic acid plays an important role in maintaining the normal function and structure of VSMCs, but high concentrations of palmitic acid can lead to osteoblastic differentiation and calcium deposition in VSMCs, and can increase oxidative stress and inflammatory responses,

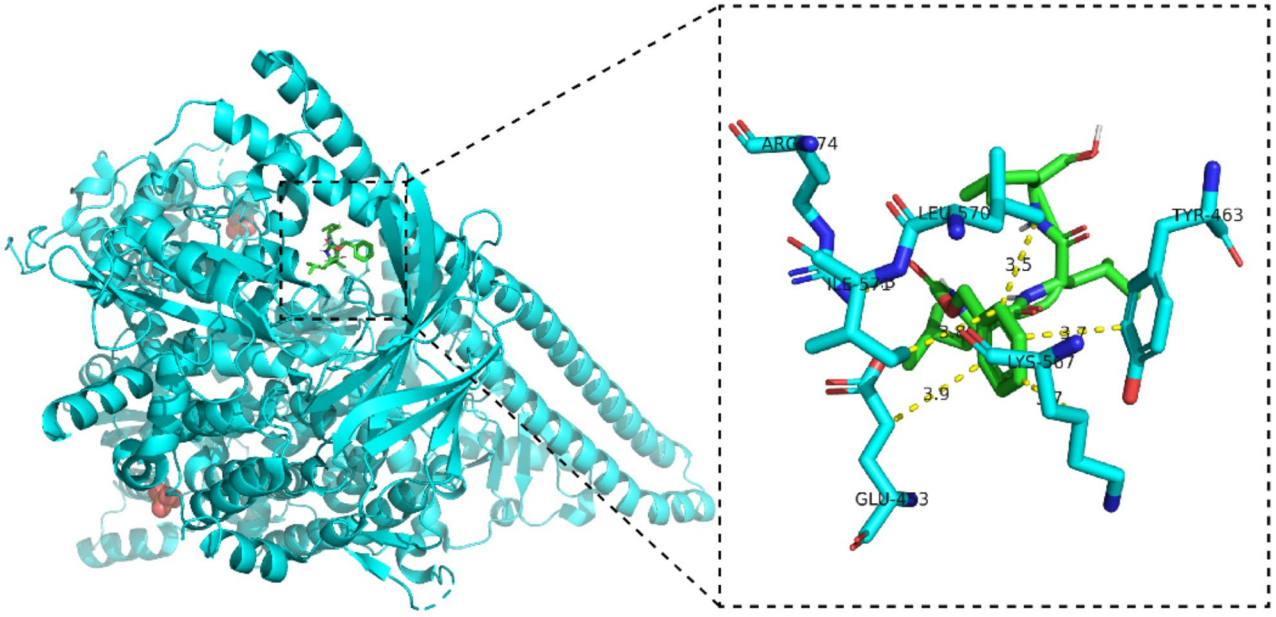

Fig. 8 Molecular docking results for MG-132 and PI3K

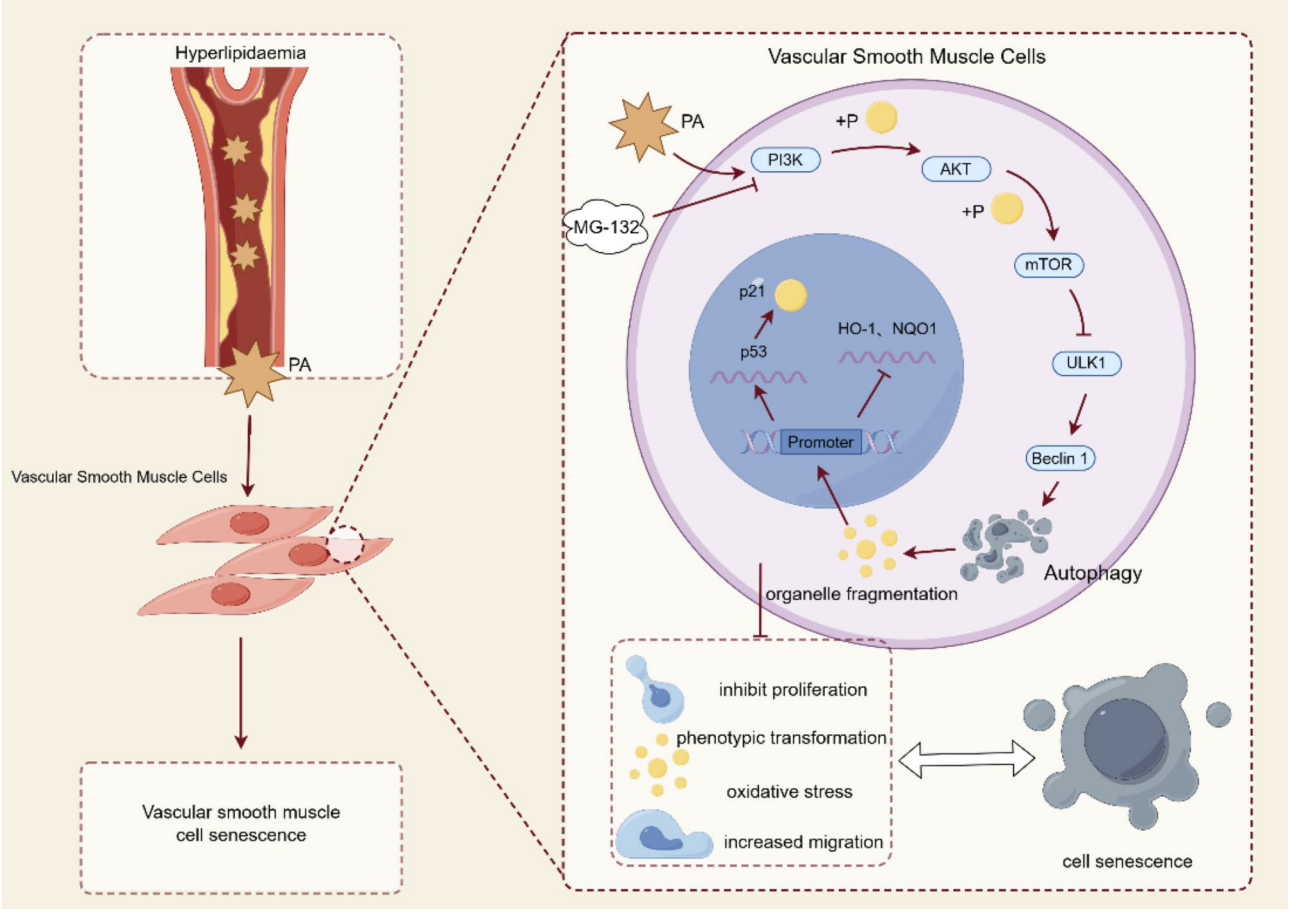

Fig. 9 Mechanism of action of MG-132 in delaying VSMC senescence

mitochondrial damage and energy metabolism disorders, as well as lipid deposition, thereby accelerating cellular senescence or death, promoting vascular sclerosis and plaque formation, and favouring the development of atherosclerosis [16, 21–25]. In addition, senescence of VSMCs may also lead to enhanced proliferation and migration, decreasing the normal repair and protective functions of the vascular wall, as well as the regulatory effects on the vascular endothelium, and increasing the susceptibility of the vascular wall to injury and inflammation [2, 26–28].The results of this study showed that the abdominal aortas of high-fat-fed mice overexpressed the senescence-related proteins p21 and p53, senescence-associated secretory phenotype (SASP) Markers (IL-1β and TNF-α), and the high-fat-induced vascular aging was significantly ameliorated by the administration of MG-132. In vitro experiments also verified our speculations, when we treated in vitro cultured VSMCs with sodium palmitate for 24 h, the level of oxidative stress and the percentage of β-galactosidase staining was both significantly increased, as did the levels of the p21 and p53, senescence-associated secretory phenotype (SASP) Markers (IL-1β and TNF-α) proteins, which are used to characterize VSMC senescence and decreased in the expression of the anti-oxidative stress-related proteins NQO1 and HO-1. After MG-132 was added, the level of oxidative stress and the percentage of β-galactosidase positive cells both significantly reduced, while inhibiting the expression of p21 and p53 and promoting the expression of NQO1 and HO-1. These findings suggest that MG-132 can inhibit oxidative stress and delay senescence in VSMCs, which may be beneficial for AS treatment.

Autophagy is an intracellular self-degradation process that involves the encapsulation of damaged or aged intracellular proteins, organelles, and other materials into VSMCs, which are then transported to lysosomes for degradation and reuse [29]. Interestingly, we found that autophagy seems to play an important role in high-fat diet-induced vascular smooth muscle senescence and therapeutic processes. Phosphatidylinositol-3 kinase (PI3K) is an essential cell signaling protein involved in the regulation of a variety of physiological processes such as cell proliferation, survival, and metabolism, and Unc-51-like autophagy activating kinase 1(ULK 1) and Beclin 1 are two key proteins in the process involved of cellular autophagy. It has been shown that the expression of ULK1 and Beclin 1 de-creases with age in animal models, implying that senescence is often accompanied by impaired autophagy [30–32]. By immunohistochemistry, we found that aortic p-PI3K was overexpressed and that the expression of ULK1 and Beclin 1 was suppressed in high-fat diet-fed mice, but the high-fat diet-induced impairment of autophagy was significantly ameliorated by MG-132 treatment. This finding suggested that high-fat diet-induced vascular senescence may be associated with impaired autophagy and that MG-132 may play a therapeutic role by activating the autophagic pathway.

To explore the mechanism of autophagy, we treated VSMCs cultured in vitro with sodium palmitate for 24 h. The results showed that the phosphorylation levels of autophagy-related proteins PI3K, AKT, and mTOR in the VSMCs induced by sodium palmitate were significantly increased, the expression levels of ULK1 and Beclin 1 were significantly decreased, the MG-132 treatment decreased the phosphorylation levels, and the expression levels of ULK1 and Beclin 1 increased. The results of cellular autophagy staining showed a significant decrease in autophagy fluorescence intensity induced by PA, and a significant increase in the fluorescence intensity of cellular autophagy staining after the addition of MG-132, suggesting that MG-132 activates autophagy in VSMCs. When Pictilisib (PI3K inhibitor) was used, the activation of autophagy was further enhanced by MG-132, which inhibited the phosphorylation of PI3K, AKT, and mTOR, while Recilisib (PI3K activator) reversed the effect of MG-132. Studies have shown that in cellular autophagy, PI3K promotes the formation of autophagic vesicles through the production of phosphatidylinositol-3 phosphate (PI3P), which forms specific structural domains on the membrane of autophagic vesicles, recruits autophagy-associated proteins, and facilitates membrane fusion and expansion of autophagic vesicles. Autophagy reduces oxidative damage and endoplasmic reticulum stress through phagocytosis and degradation; thus, the promotion of autophagy improves cellular antioxidant capacity, and reduces DNA damage and inflammatory responses [33–37]. mTOR, a mammalian target of rapamycin, is a recognized downstream signaling molecule of AKT can directly affects the initiation and execution of cellular autophagy by regulating the phosphorylation status of ULK1. This detailed regulatory mechanism ensures that cells can flexibly adjust their autophagic activities under different environmental conditions to maintain intracellular homeostasis and adapt to the demands of the external environment. In conclusion, our results revealed that MG-132 inhibited the PA-induced aberrant proliferation and migration of VSMCs, reduced the level of oxidative stress, and delayed senescence in association with the reduced activity of the PI3K/AKT/mTOR pathway and activation of cellular autophagy. The molecular docking technique also theoretically demonstrated that the ligand carbon atom of MG-132 could form strong hydrophobic interactions with the PI3K amino acid residues GLU, TYR, LYS, LEU, and ILE, and at the same time, MG-132 could provide an acceptor to form a hydrogen bond with the donor provided by ARG, which verified the targeting relationship between MG-132 and PI3K. However, there are limitations to this study, firstly, the relationship

between autophagy and senescence also needs to be further clarified, and secondly, the mechanism of action of MG-132 is multifaceted and may involve various cellular pathways other than senescence and autophagy. Future studies could further enhance the exploration of the relationship between autophagy and senescence, as well as the specific molecular targets and downstream effects of MG-132 treatment, in order to fully understand its impact on vascular biology.

In conclusion, it can be concluded that MG-132 activates sodium palmitate-induced autophagy in human vascular smooth muscle cells and inhibits senescence via the PI3K/AKT/mTOR axis.

Supplementary Information

The online version contains supplementary material available at https://doi.org/10.1186/s12944-024-02268-w.

Supplementary Material 1

Supplementary Material 2

Supplementary Material 3

Author contributions

Zhiyun Shu: experimental design and data collection, Xiangjun Li: data analysis and interpretation of results, Wenqing Zhang: literature review and background research, Zixu Huyan: experimental design and data processing, Dong Cheng: maintenance and calibration of experimental equipment, Shishun Xie: data analysis and graphing. Hongyuan Cheng: experimental process supervision and quality control, Jiajia Wang: discussion section writing and future research direction, Bing Du: full text writing and final approval. Each of the authors played an important role in the writing of this article and worked together to complete this research work.

Funding

This work was supported by the 'Natural Science Foundation of Jilin Province' (Grant No. YDZJ202201ZYTS036 to Du Bing and Grant No. 20210101316JC to Li Xiangjun).

Data availability

No datasets were generated or analysed during the current study.

Declarations

Ethical approval

The ethics of animal experimentation in this study was approved by the Ethics Committee for Animal Experimentation of the First Hospital of Jilin University, No.0845.The experiments were conducted in accordance with the Regulations on the Management of Experimental Animals, which stipulate the ethical guidelines and operational practices that must be followed in animal experiments.

Competing interests

The authors declare no competing interests.

Received: 31 March 2024 / Accepted: 19 August 2024
Published online: 04 September 2024

References

1. Chistiakov DA, Orekhov AN, Bobryshev YV. Vascular smooth muscle cell in atherosclerosis[J]. Acta Physiol 2015, 214(1): 33–50.
2. Wang J, Uryga AK, Reinhold J et al. Vascular smooth muscle cell senescence promotes atherosclerosis and features of Plaque Vulnerability[J]. Circulation,2015, 132(20): 1909–19.
3. Grootaert MOJ, Moulis M, Roth L, et al. Vascular smooth muscle cell death, autophagy and senescence in atherosclerosis[J]. Cardiovascular Res. 2018;114(4):622–34.
4. Feng Y, He D, Yao Z, et al. The machinery of macroautophagy[J]. Cell Res. 2014;24(1):24–41.
5. Nepstad I, Hatfield KJ, Grønningsæter IS et al. The PI3K-Akt-mTOR signaling pathway in human acute myeloid leukemia (AML) Cells[J]. Int J Mol Sci 2020, 21(8): 2907.
6. Ersahin T, Tuncbag N, Cetin-Atalay R. The PI3K/AKT/mTOR interactive pathway[J]. Mol Biosyst. 2015;11(7):1946–54.
7. Yu L, Wei J, Liu P. Attacking the PI3K/Akt/mTOR signaling pathway for targeted therapeutic treatment in human cancer[J]. Seminars Cancer Biology 2022, 85: 69–94.
8. Gao Y, Zhang Y, Fan Y. Eupafolin ameliorates lipopolysaccharide-induced cardiomyocyte autophagy via PI3K/AKT/mTOR signaling pathway[J]. Iran J Basic Med Sci,2019, 22(11).
9. Hou X, Hu Z, Xu H, et al. Advanced glycation endproducts trigger autophagy in cadiomyocyte Via RAGE/PI3K/AKT/mTOR pathway[J]. Cardiovasc Diabetol. 2014;13(1):78.
10. Xia Q, Xu M, Zhang P et al. Therapeutic potential of Autophagy in Glioblastoma Treatment with Phosphoinositide 3-Kinase/Protein kinase B/Mammalian target of Rapamycin Signaling Pathway Inhibitors[J]. Frontiers in Oncology,2020, 10: 572904.
11. Grootaert MO, Da Costa Martins PA, Bitsch N et al. Defective autophagy in vascular smooth muscle cells accelerates senescence and promotes neointima formation and atherogenesis[J]. Autophagy,2015, 11(11): 2014–32.
12. LaRocca TJ, Gioscia-Ryan RA, Hearon CM, et al. The autophagy enhancer spermidine reverses arterial aging[J]. Mech Ageing Dev. 2013;134(7–8):314–20.
13. Salabei JK, Hill BG. Implications of autophagy for vascular smooth muscle cell function and plasticity[J]. Free Radic Biol Med. 2013;65:693–703.
14. Harhouri K, Navarro C, Depetris D et al. MG 132-induced progerin clearance is mediated by autophagy activation and splicing regulation[J]. EMBO Mol Med 2017, 9(9): 1294–313.
15. Kong P, Cui Z-Y, Huang X-F et al. Inflammation and atherosclerosis: signaling pathways and therapeutic intervention[J]. Signal Transduct Target Therapy 2022, 7(1): 131.
16. Wu D, Liu J, Pang X et al. Palmitic acid exerts pro-inflammatory effects on vascular smooth muscle cells by inducing the expression of C-reactive protein, inducible nitric oxide synthase and tumor necrosis factor-α[J]. Int J Mol Med 2014, 34(6): 1706–12.
17. Titov VN, Kukharchuk VV. [The integrated etiology and separate pathogenesis of atherosclerosis and atheromatosis. The differences of fatty acids transfer in lipoproteins of herbivorous and carnivorous animals.][J]. Klinicheskaia laboratornaia diagnostika,2017, 62(4): 196–204.
18. Titov VN, Rozhkova TA, Kaminnaya VA et al. [Atherosclerosis and atheromatosis are consequtive metabolic disordes. Pathology of the biological functions of trophology and endoecology is the basis for ischemic heart disease prevention.][J]. Klinicheskaia laboratornaia diagnostika,2018, 63(4): 196–204.
19. Jin F, Jiang S, Yang D et al. Acipimox attenuates atherosclerosis and enhances plaque stability in ApoE-deficient mice fed a palmitate-rich diet[J]. Biochem Biophys Res Commun 2012, 428(1): 86–92.
20. Afonso MS, Lavrador MSF, Koike MK et al. Dietary interesterified fat enriched with palmitic acid induces atherosclerosis by impairing macrophage cholesterol efflux and eliciting inflammation[J]. J Nutritional Biochem 2016, 32: 91–100.
21. Brodeur MR, Bouvet C, Barrette M et al. Palmitic acid increases medial calcification by inducing oxidative Stress[J]. J Vascular Res 2013, 50(5): 430–41.
22. Raman P, Madhavpeddi L, Gonzales RJ. Palmitate induces glycosylation of cyclooxygenase-2 in primary human vascular smooth muscle cells[J]. Am J Physiology-Cell Physiol 2018, 314(5): C545–53.
23. Chen Z, Sun X, Li X et al. Oleoylethanolamide alleviates hyperlipidaemia-mediated vascular calcification via attenuating mitochondrial DNA stress triggered autophagy-dependent ferroptosis by activating PPARα[J]. Biochemical Pharmacology,2023, 208: 115379.
24. Peng Z, Tan X, Xie L et al. PKR deficiency delays vascular aging via inhibiting GSDMD-mediated endothelial cell hyperactivation[J]. iScience,2023, 26(1): 105909.
25. Kageyama A, Matsui H, Ohta M, et al. Palmitic acid induces osteoblastic differentiation in vascular smooth muscle cells through ACSL3 and NF-κB, novel

targets of Eicosapentaenoic Acid[J]. Volume 8. MOHANRAJ R. PLoS ONE; 2013. p. e68197. 6.
26. Xia Y, Zhang X, An P et al. Mitochondrial homeostasis in VSMCs as a Central Hub in Vascular Remodeling[J]. Int J Mol Sci 2023, 24(4): 3483.
27. Hénaut L, Mary A, Chillon J-M et al. The impact of Uremic toxins on vascular smooth muscle cell Function[J]. Toxins,2018, 10(6): 218.
28. Lin M-J, Hu S-L, Tian Y et al. Targeting vascular smooth muscle cell senescence: a Novel Strategy for Vascular Diseases[J]. J Cardiovasc Translational Res 2023, 16(5): 1010–20.
29. Doherty J, Baehrecke EH. Life, death and autophagy[J]. Nat Cell Biology 2018, 20(10): 1110–7.
30. Triplett JC, Tramutola A, Swomley A et al. Age-related changes in the proteostasis network in the brain of the naked mole-rat: implications promoting healthy longevity[J]. Biochimica et Biophysica Acta (BBA) - molecular basis of Disease,2015, 1852(10): 2213–24.
31. Lipinski MM, Zheng B, Lu T et al. Genome-wide analysis reveals mechanisms modulating autophagy in normal brain aging and in Alzheimer's disease[J]. Proceedings of the National Academy of Sciences,2010, 107(32): 14164–14169.
32. Yu Y, Feng L, Li J, et al. The alteration of autophagy and apoptosis in the hippocampus of rats with natural aging-dependent cognitive deficits[J]. Behav Brain Res. 2017;334:155–62.
33. Malemud CJ. The PI3K/Akt/PTEN/mTOR pathway: a fruitful target for inducing scell death in rheumatoid arthritis?[J]. Future Med Chem 2015, 7(9): 1137–47.
34. Xie S, Chen M, Yan B et al. Identification of a role for the PI3K/AKT/mTOR signaling pathway in Innate Immune Cells[J]. RYFFEL B PLoS ONE 2014, 9(4): e94496.
35. Qazi A, Hussain A, Hamid A et al. Recent development in Targeting PI3K-Akt-mTOR signaling for Anticancer therapeutic Strategies[J]. Anti-Cancer Agents Med Chem 2013, 13(10): 1552–64.
36. Pharmacodynamic Biomarker Development for PI3K Pathway Therapeutics[J]. Translational Oncogenomics 2016 Suppl 1: 33–49.
37. Alers S, Löffler AS, Wesselborg S et al. Role of AMPK-mTOR-Ulk1/2 in the regulation of Autophagy: Cross Talk, Shortcuts, and Feedbacks[J]. Mol Cell Biology 2012, 32(1): 2–11.

Publisher's note